

Quantum Tunneling of Magnetization in a New $[\text{Mn}_{18}]^{2+}$ Single-Molecule Magnet with $S = 13$

Euan K. Brechin,[†] Colette Boskovic,[†] Wolfgang Wernsdorfer,[‡] Jae Yoo,[§] Akira Yamaguchi,[#]
E. Carolina Sañudo,[†] Thomas R. Concolino,^{||} Arnold L. Rheingold,^{||} Hidehiko Ishimoto,[#]
David N. Hendrickson,^{*,§} and George Christou^{*,†,⊥}

Department of Chemistry, Indiana University, Bloomington, Indiana 47405-7102, Laboratoire Louis Néel-CNRS, 38042 Grenoble, Cedex 9, France, Department of Chemistry-0358, University of California at San Diego, La Jolla, California 92093-0358, Institute for Solid State Physics, University of Tokyo, 7-22-1 Roppongi, Minatoku, Tokyo 106-8666, Japan, and Department of Chemistry, University of Delaware, Newark, Delaware 19716

Received April 3, 2002

Many present and future specialized applications of magnets require monodisperse, nanoscale magnetic particles, and the discovery that individual molecules can function as nanoscale magnets was thus a significant development.^{1–3} Such a molecule, named a single-molecule magnet (SMM), functions as a single-domain magnetic particle that, below its blocking temperature, exhibits the classical property of a magnet, namely, magnetization hysteresis. In addition, it straddles the classical/quantum interface in also displaying quantum tunneling of magnetization (QTM)⁴ and quantum phase interference.⁵ A SMM derives its unusual properties from a combination of large spin (S) and large, easy-axis-type anisotropy (negative axial zero-field splitting parameter D). These result in a significant barrier to thermally activated magnetization relaxation, with upper limits given by $S^2|D|$ or $(S^2 - 1/4)|D|$ for integer and half-integer spin, respectively. The first SMM was $[\text{Mn}_{12}\text{O}_{12}(\text{O}_2\text{CMe})_{16}(\text{H}_2\text{O})_4]^{1-3}$ with $S = 10$ and $D = -0.50 \text{ cm}^{-1} = -0.72 \text{ K}$. Since then, other oxidation levels of the $[\text{Mn}_{12}]$ family⁶ and other Mn_x and M_x ($M = \text{Fe}, \text{V}, \text{Ni}$) SMMs have been prepared with various S values, both integer and half-integer.⁷ Recently, the first exchange-coupled dimer of SMMs has demonstrated the feasibility of fine-tuning the quantum properties of these nanoscale magnetic materials.⁸

We herein report a new $[\text{Mn}_{18}]^{2+}$ SMM with a particularly large spin of $S = 13$. In addition, it undergoes QTM and is both the largest spin and the highest nuclearity SMM to exhibit this quantum behavior. It thus represents a particularly valuable addition to the SMM family.

A solution of $[\text{Mn}_3\text{O}(\text{O}_2\text{CMe})_6(\text{py})_3](\text{ClO}_4)$ and $[\text{Mn}_3\text{O}(\text{O}_2\text{CMe})_6(\text{py})_3]\cdot\text{py}$ (2:1) in MeCN was treated with hepH (2-(hydroxyethyl)pyridine; ~ 4.5 equiv). After 18 h, the filtered solution was carefully layered with Et₂O, and it slowly produced black crystals of $[\text{Mn}_{18}\text{O}_{14}(\text{O}_2\text{CMe})_{18}(\text{hep})_4(\text{hepH})_2(\text{H}_2\text{O})_2](\text{ClO}_4)_2$ (**1**) as **1**·6MeCN in 10% yield. Vacuum-dried solid analyzed as solvent-free.⁹ The structure¹⁰ reveals a centrosymmetric cation (Figure 1) whose $[\text{Mn}_{18}(\mu_4\text{-O})_4(\mu_3\text{-O})_{12}(\mu\text{-O})_8]^{4+}$ core comprises a central, near-linear Mn_4O_6 unit (Mn1, Mn1', Mn6, Mn6'), to either side of which is attached a Mn_7O_9 unit. Six of the bridging O atoms in the $\text{Mn}_{18}\text{O}_{24}$ core are from hep⁻/hepH groups and four are from MeCO_2^- groups; the rest are O^{2-} ions. Close examination of metric parameters reveals O27 and O27' to be protonated (i.e., hepH). Bond valence

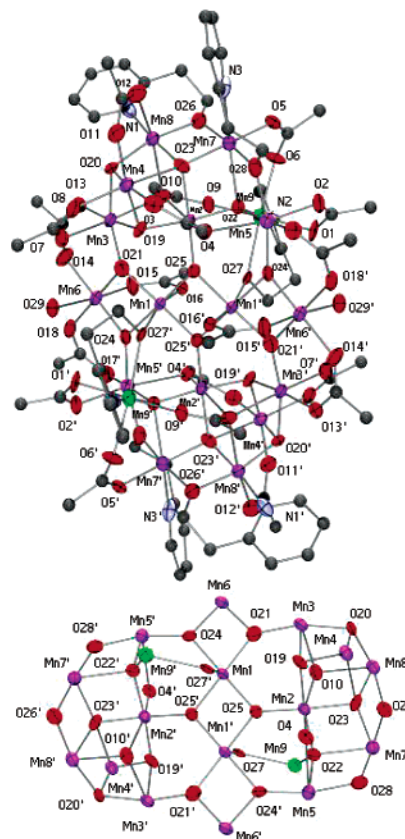


Figure 1. Labeled PovRay plots at 50% probability for the cation of **1** and its $\text{Mn}_{18}\text{O}_{24}$ core: Mn^{3+} purple; Mn^{2+} green; O red; N blue; C black.

sums and Jahn–Teller elongation axes establish a $2\text{Mn}^{\text{II}}, 16\text{Mn}^{\text{III}}$ trapped-valence oxidation state description, with Mn9 and Mn9' being the Mn^{II} ions.

The ground-state spin of **1** was determined by solid-state magnetization measurements in the 2.0–4.0 K and 20–50 kG ranges (Figure 2). The data were fit by diagonalization of the spin Hamiltonian matrix using a full powder-average method that assumes only the ground state is populated and incorporates axial ZFS ($D\hat{S}_z^2$) and Zeeman interactions. The fit (solid line) gave $S = 13$, $D = -0.13 \text{ cm}^{-1} = -0.19 \text{ K}$, and $g = 1.86$. Although a few higher spin values are known, $S = 13$ is nevertheless an unusually large spin for a molecular species. Its calculated barrier to relaxation ($S^2|D|$) is 32 cm^{-1} (46 K), suggesting **1** might be a new SMM. This was therefore investigated.

* Address correspondence to this author. E-mail: christou@chem.ufl.edu.

[†] Indiana University.

[‡] Laboratoire Louis Néel.

[§] University of California.

[#] University of Tokyo.

^{||} University of Delaware.

[⊥] Present address: University of Florida.

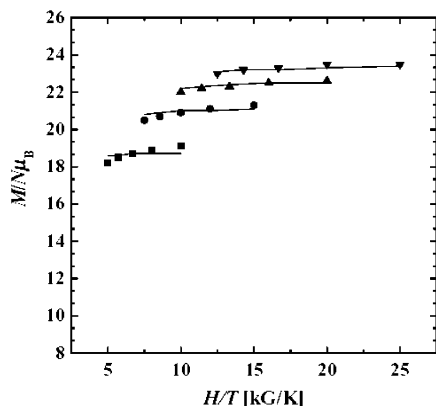


Figure 2. Plot of reduced magnetization, $(M/N\mu_B)$ vs H/T for **1** at 50 (∇), 40 (\blacktriangle), 30 (\bullet), and 20 (\blacksquare) kG. The solid lines are the fit; see the text for the fitting parameters.

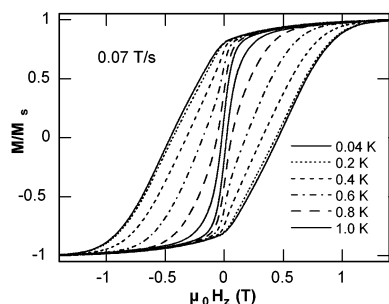


Figure 3. Magnetization (M) vs field hysteresis loops for **1** at the indicated temperatures. M is normalized to its saturation value, M_s .

AC susceptibility data were collected in the 0.04–4.0 K range at nine frequencies from 1.1 to 996 Hz. Frequency-dependent out-of-phase AC susceptibility (χ'') signals were observed in the 0.99–1.44 K region, indicating the superparamagnet-like slow relaxation of a SMM. To confirm this, magnetization vs applied DC field data were collected down to 0.04 K using a micro-SQUID instrument. Hysteresis loops were observed below 1 K whose coercivities increase with decreasing temperature (Figure 3), as expected for a SMM. The loops do not show the steplike features indicative of QTM, but it is possible that steps are present but smeared out by broadening effects from dipolar and transverse fields, intermolecular interactions, and/or a distribution of molecular environments.

To probe whether **1** is undergoing QTM and to determine the effective barrier to magnetization relaxation (U_{eff}), DC magnetization decay data were collected (i) on a microcrystalline sample using a SHE-RM bridge where a SQUID serves as a null detector; a field of 3.7 G was applied and after temperature equilibration, the field was removed and the magnetization measured as a function of time at 11 temperatures in the 0.910–0.080 K range, with data collection times up to 10^5 s at 0.080 K, and (ii) on a single crystal at 16 temperatures in the 0.040–1.00 K range using a micro-SQUID instrument. Each of the 27 data sets was analyzed to give a relaxation time (τ).

The DC decay and AC χ'' data were combined and used to construct an Arrhenius plot of $\ln \tau$ vs $1/T$ (Figure 4). Between 3.50 and 0.50 K, the relaxation rate is temperature-dependent with $U_{\text{eff}} = 14.8 \text{ cm}^{-1} = 21.3 \text{ K}$, likely as a result of a thermally activated (Orbach) process.¹¹ However, below ca. 0.25 K, the relaxation rate is temperature-independent at $1.3 \times 10^{-8} \text{ s}^{-1}$, indicative of QTM

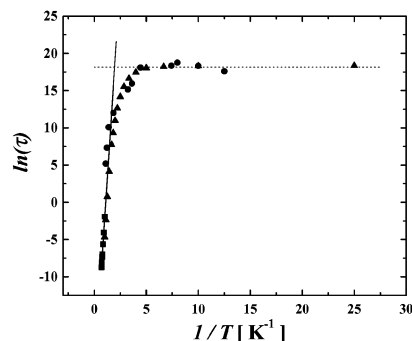


Figure 4. Arrhenius plot for **1** using AC χ'' data (\blacksquare) and DC decay data on single-crystal (\blacktriangle) and microcrystalline (\bullet) samples. The solid line is the fit of the data in the thermally activated region, and the dashed line is the fit of the temperature-independent data.

between the lowest energy $M_s = \pm 13$ levels of the $S = 13$ state. Such temperature-independent relaxation rates have been reported previously for only a few SMMs.^{7a,d,12,13}

In summary, the new $[\text{Mn}_{18}]^{2+}$ cluster **1** is among the largest spin ($S = 13$) and size SMMs to be discovered. In addition, it is both the largest spin and highest nuclearity SMM to exhibit quantum tunneling of magnetization.

Acknowledgment. This work was supported by NSF grants to G.C. and D.N.H.

Supporting Information Available: Crystallographic details (CIF) for **1**-6MeCN. This material is available free of charge via the Internet at <http://pubs.acs.org>.

References

- (1) Christou, G.; Gatteschi, D.; Hendrickson, D. N.; Sessoli, R. *MRS Bulletin* **2000**, 25, 66–71.
- (2) Sessoli, R.; Tsai, H.-L.; Schake, A. R.; Wang, S.; Vincent, J. B.; Folting, K.; Gatteschi, D.; Christou, G.; Hendrickson, D. N. *J. Am. Chem. Soc.* **1993**, 115, 1804.
- (3) Sessoli, R.; Gatteschi, D.; Caneschi, A.; Novak, M. A. *Nature* **1993**, 365, 141.
- (4) Friedman, J. R.; Sarachik, M. P.; Tejada, J.; Ziolo, R. *Phys. Rev. Lett.* **1996**, 76, 3830.
- (5) Wernsdorfer, W.; Sessoli, R. *Science* **1999**, 284, 133–135.
- (6) (a) Eppley, H. J.; Tsai, H.-L.; de Vries, N.; Folting, K.; Christou, G.; Hendrickson, D. N. *J. Am. Chem. Soc.* **1995**, 117, 301. (b) Soler, M.; Chandra, S. K.; Ruiz, D.; Davidson, E. R.; Hendrickson, D. N.; Christou, C. *Chem. Commun.* **2000**, 2417–2418.
- (7) (a) Hendrickson, D. N.; Christou, G.; Ishimoto, H.; Yoo, J.; Brechin, E. K.; Yamaguchi, A.; Rumberger, E. M.; Aubin, S. M. J.; Sun, Z.; Aromi, G. *Polyhedron* **2001**, 20, 1479 and references therein. (b) Boskovic, C.; Brechin, E. K.; Streib, W. E.; Folting, K.; Bollinger, J. C.; Hendrickson, D. N.; Christou, G. *J. Am. Chem. Soc.* **2002**, 124, 3725. (c) Soler, M.; Rumberger, E.; Folting, K.; Hendrickson, D. N.; Christou, G. *Polyhedron* **2001**, 20, 1365. (d) Cadiou, C.; Murrie, M.; Paulsen, C.; Villar, V.; Wernsdorfer, W.; Winpenny, R. E. P. *Chem. Commun.* **2001**, 2666.
- (8) Wernsdorfer, W.; Aliaga-Alcalde, N.; Hendrickson, D. N.; Christou, G. *Nature* **2002**, 416, 406.
- (9) Elemental analysis calcd (found) for $\text{C}_{78}\text{H}_{108}\text{Cl}_2\text{Mn}_{18}\text{N}_6\text{O}_{66}$: C, 28.87 (29.00); H, 3.35 (3.25); N, 2.59 (2.61).
- (10) Crystal data for **1**-6MeCN: $\text{C}_{90}\text{H}_{126}\text{Cl}_2\text{Mn}_{18}\text{N}_{12}\text{O}_{66}$, 3491.83 g mol^{-1} , triclinic, $P1$, $a = 13.4785(3)$, $b = 15.4119(4)$, $c = 17.7509(4)$ Å, $\alpha = 89.8405(8)$, $\beta = 77.7478(7)$, $\gamma = 66.4181(11)^\circ$, $Z = 1$, $V = 3288.6$ Å³, $d_{\text{calc}} = 1.762$ g cm^{-3} , $T = -50$ °C. The structure was solved by direct methods and refined on F^2 . An empirical absorption correction was performed (DIFABS). Hydrogen atoms were included in fixed, calculated positions. The final R1 and wR2 were 13.88% and 29.82%, respectively.
- (11) Abragam, A.; Bleaney, B. *Electron Paramagnetic Resonance of Transition Ions*; Dover Press: Minneaola, NY, 1986.
- (12) Sangregorio, C.; Ohm, T.; Paulsen, C.; Sessoli, R.; Gatteschi, D. *Phys. Rev. Lett.* **1997**, 78, 4645.
- (13) Aubin, S. M. J.; Dilley, N. R.; Pardi, L.; Krzystek, J.; Wemple, M. W.; Brunel, L.-C.; Maple, M. B.; Christou, G.; Hendrickson, D. N. *J. Am. Chem. Soc.* **1998**, 120, 4991.

JA026407G